Water Research 213 (2022) 118149

Contents lists available at ScienceDirect

Water Research

journal homepage: www.elsevier.com/locate/watres

An online flow-imaging particle counter and conventional water quality sensors detect drinking water contamination in the presence of normal water quality fluctuations

Markus Koppanen [a,*], Tero Kesti [b], Marika Kokko [a], Jukka Rintala [a], Marja Palmroth [a]

[a] Faculty of Engineering and Natural Sciences, Tampere University, P.O. Box 541, FI-33101, Tampere, Finland
[b] Uponor Corporation, Kaskimäenkatu 2, FI-33900 Tampere, Finland

ARTICLE INFO

Keywords:
Online particle counting
Water quality monitoring
Contamination detection
Drinking water distribution
Flow imaging

ABSTRACT

Contamination detection in drinking water is crucial for water utilities in terms of public health; however, current online water quality sensors can be unresponsive to various possible contaminants consisting of particulate and dissolved content or require a constant supply of reagents and sample preparation. We used a two-line test environment connected to a drinking water distribution system with flow-imaging particle counters and conventional sensors to assess their responses to the injection of contaminants into one line, including stormwater, treated wastewater, wastewater, well water, and *Escherichia coli*, while simultaneously measuring responses to normal water quality fluctuations in the other line. These water quality fluctuations were detected with all of the conventional sensors (except conductivity) and with 3 out of 5 of the size- and shape-derived particle classes of the flow-imaging particle counter. The flow-imaging particle counter was able to detect all of the studied contaminants, e.g. municipal wastewater at 0.001% (v/v), while the oxidation–reduction potential sensor outperformed other conventional sensors, detecting the same wastewater at 0.03% (v/v). The presence of particles less than 1 μm in size was shown to be a generic parameter for the detection of particulates present in the studied contaminants; however, they manifested a considerable response to fluctuations which led to lower relative response to contaminants in comparison to larger particles. The particle size and class distributions of contaminants were different from those of drinking water, and thus monitoring particles larger than 1 μm or specific particle classes of flow-imaging particle counter, which are substantially more abundant in contaminated water than in pure drinking water, can improve the detection of contamination events. Water utilities could optimize contamination detection by selecting water quality parameters with a minimal response to quality fluctuations and/or a high relative response to contaminants.

1. Introduction

Contamination in drinking water can cause public health and economic consequences. Such contamination can occur in the production and distribution stages of the water supply via various pathways, including raw water quality impairments (Whelton et al., 2015), treatment deficiencies (Rhoads et al., 2017), and failures in the distribution system (DS) (Besner et al., 2011). Examples of contamination pathways include wastewater discharge or surface runoff entering the raw water source (Larsson et al., 2014; Mellou et al., 2014), treated wastewater entering the DS from a cross-connection (Laine et al., 2011), and wastewater, surface runoff, or groundwater in the proximity of drinking water infrastructure of low physical integrity, intruding into the DS when pressure transients are present (Besner et al., 2011). The contamination is likely to increase particulate and dissolved content in the contaminated water. To prevent these external contaminants from reaching water consumers, an early warning system (EWS) can be established that utilizes online water quality sensors and algorithms to detect contamination among normal water quality variations in the DS (Liu et al., 2015).

Conventional online water quality sensors used in water treatment plant process monitoring, and also considered for routine DS monitoring as well as for EWS, measure parameters such as turbidity, conductivity, chlorine concentration, and pH (Liu et al., 2014). Even though the

* Corresponding author.
E-mail address: markus.koppanen@tuni.fi (M. Koppanen).

https://doi.org/10.1016/j.watres.2022.118149
Received 4 October 2021; Received in revised form 20 December 2021; Accepted 31 January 2022
Available online 2 February 2022

performance of conventional online water quality sensors has been deemed sufficient for EWS (Liu et al., 2016), many of these sensors, such as those for measuring pH and conductivity, are more likely to detect dissolved than particulate contaminants. In addition, conventional online water quality sensors cannot determine the characteristics of particulate content. For example, turbidity is a sum parameter for particulate content, but it does not provide information on the number of particles, their size distribution, or whether they are microbes or chemical precipitates (Pronk et al., 2007).

Since many potential contamination scenarios in DS include particles such as microbes and chemical precipitates or their aggregates, the need for accurate and reliable particulate monitoring is evident. For that reason, the recent emergence of optical, counting-based online technologies has been studied for their capacity to monitor suspended particles at high frequency in DS, including online flow cytometry (Safford and Bischel, 2019) and online flow-imaging-based particle counting (Højris et al., 2018, 2016). Flow imaging involves the capture of images of flowing water at a certain volume through a microscope and data analysis methods to analyze the images for the size and form of particles (Ripple and DeRose, 2018). On the other hand, flow cytometry forces suspended particles, pre-stained with reagents, into a single file and measures the scattered light and/or fluorescence with a laser beam (Safford and Bischel, 2019). Comparing these two technologies, selective staining in flow cytometry requires reagents and incubation and can be used to qualitatively distinguish cells and their viability and activity among other particulate material (Safford and Bischel, 2019), while flow imaging can be used to estimate the total cell count (TCC) by classifying particles according to their morphology in addition to particle size distribution with no additional reagents or sample preparation (staining and incubation) (Højris et al., 2016). Thus, flow imaging is expected to result in less frequent maintenance and higher measurement frequency. For instance, Højris et al. (2016) presented an online flow-imaging method based on dark-field microscopy that classifies particle images into abiotic particles and bacteria. The present study introduces a novel online flow-imaging particle counter based on lensless digital inline holographic microscopy (DIHM), which classifies particles by machine-learned features not typical in drinking water and by their size. When compared to conventional microscopy using a magnifying objective, lensless DIHM allows much larger water volumes to be measured because of the considerably larger field of view and depth of field of a single image and the ability to take images in rapid succession in a flow cell arrangement (Ozcan and McLeod, 2016; Xu et al., 2001).

EWS require information on the detection performance of sensors to set correct levels of alarm. The development of contamination detection methods typically occurs using pilot-scale test environments in which contaminants are injected into drinking water without the risk of contaminating the DS. These studies commonly use tap water as a source of drinking water. However, drinking water quality normally varies in a DS and may result in fluctuations in a signal of a measured parameter (Hall et al., 2007), which should be taken into account by determining a baseline signal. Pilot-scale studies reduce the presence of these quality fluctuations by pre-collecting water in large tanks ($>$ 1000 L) before conveying it to the test environment (Dejus et al., 2018; Ikonen et al., 2017) or recirculating the water to establish a stable baseline (Hall et al., 2007; Helbling and VanBriesen, 2008). McKenna et al. (2008) suggested that the water quality fluctuations in similar pilot-scale test environments may be considerably smaller than the quality fluctuations in the actual DS, thereby possibly overestimating sensor performance in contaminant detection in natural conditions.

The present study considered the water quality changes arising both from injected contaminants and from normal water quality fluctuations in a DS by monitoring the water quality simultaneously from two identical measurement lines. By subtracting the response of the sensors in the line measuring normal water quality fluctuations (later referred to as "reference line") from that of the sensors in the line measuring injected contaminants (later referred to as "contamination line"), the water quality change caused by the contaminant alone was obtained. The aim of the present study was to evaluate the responses of a novel flow-imaging particle counter and conventional water quality sensors to fluctuating drinking water quality and real-life contaminants including stormwater, treated wastewater, wastewater, and well water in addition to *Escherichia coli (E. coli),* in the DS. An ideal sensor would have a far greater response for a real contamination than for normal water quality fluctuations; thus, the secondary aim was to study whether particle characteristics can be utilized to improve contamination detection. Due to the vast amount of recorded data, the present work highlights the most considerable observations by examples.

2. Materials and methods

2.1. Test environment

The test environment was connected via a tap to the drinking water DS at Tampere University, Hervanta Campus (Tampere, Finland). In this test environment, eight sets of contaminant injections, referred to as contamination experiments, were introduced to drinking water by means of a continuously running test environment in the study period, namely summer and autumn 2020 (Jun 2nd – Jul 16th, Sep 21st – Nov 26th). The water mainly originated from the Rusko surface water treatment plant (produces ca. 13 million m^3 annually) operated by Tampere Water, which uses Lake Roine as a raw water source. The treatment plant is approximately 2 km away from the university. The variation in drinking water quality in 24-hour periods on the contamination experiment days is shown in Table 1. The free chlorine concentration varied between 0.19 and 0.31 mg/L.

The test environment consisted of a contamination line and reference line, both including a feed container (10 L, polypropylene) and a mixing container (diameter 110 mm, height 600 ±3 mm, polypropylene), followed by a line for the flow-imaging particle counter and light-scattering particle counter (contamination line only) and a sensor rack for the conventional online water quality sensors (diameter 50 mm, polypropylene) (Fig. 1). In the mixing container, the drinking water was mixed with the selected contaminant or reference feed during the contamination experiments while including an air gap to prevent backflow and an air hole to maintain atmospheric pressure in the containers. The reference feed was drinking water, except in the *E. coli* experiment, in which drinking water diluted phosphate buffered saline (PBS) was used instead.

Between the contamination experiments, only the drinking water flowed through the mixing containers. Water flowed gravitationally out of the mixing containers since the water level in the containers was approximately 245 cm higher than the end of the effluent tube in the test environment. The water level of the mixing containers was held constant by water level sensors that were connected to a control system based on a microcontroller (Leonardo, Arduino, USA) and electric solenoid valves (Geoline MY18 40 bar, Tecomec, Italy). The flow in the lines was adjusted to approximately 5500 mL/min via a half-inch manual ball valve. The flow was measured by ultrasound flow sensors (UF08B, Cynergy3, UK). During the contaminant injections, the contaminant and reference feeds were injected into the corresponding mixing containers by a single peristaltic pump (tube inner diameter, 3.1 mm) at 300 mL/min. The retention time from the feed containers to the sensors was approximately 1 min, as confirmed by injecting sodium chloride from the feed container and monitoring the increase of conductivity (results not shown), thus minimizing the warming of the drinking water. The test environment was qualified by determining the efficient mixing for particles up to 6 μm in size and ensuring that the contamination and reference line had similar TCC concentration prior to the contamination experiments (for details, see **S1 Text S1-S2**).

Table 1
Characteristics of effluent of the test environment prior to the contamination experiments (i.e. drinking water) and characteristics of filtered contaminants. The drinking water characteristics of the eight contamination experiments are shown as the mean range. The characteristics of the filtered contaminants and *Escherichia coli* (*E. coli*) are shown as means with standard deviations.

Studied water	Sample storing time (days)	pH	Oxidation reduction potential (mV)	Conductivity (μS/cm)	Turbidity (NTU)	Total suspended solids (mg/L)	Dissolved organic carbon (mg/L)	Total cell count (cells/mL)
Drinking water	0	7.79–8.22	582–719	150.3–157.4	0.05–0.24	n.d.	1.6–2.8	8300 - 81,000
Stormwater A	1	6.71 ± 0.01	n.d.	134.1 ± 0.3	77.20 ± 1.43	29 ± 2	40.9 ± 1.2	n.d.
Stormwater B	8	7.11±0.01	356±3	120.1 ± 0.1	68.47 ± 9	18 ± 1	n.d.	n.d.
Treated wastewater A	0	7.81 ± 0.02	325±3	970.7 ± 1.5	1.69 ± 0.03	n.d.	13.4 ± 0.2	n.d.
Treated wastewater B	0	7.71 ± 0.00	223±9	951.0 ± 0.0	3.89 ± 0.13	4 ± 0.4	9.6 ± 0.1	2 200 000 ± 41 000
Wastewater A	0	7.53 ± 0.02	n.d.	755.7 ± 1.53	117.90 ± 0.6	164 ± 9	50.4 ± 8.5	24 000 000 ± 4 900 000
Wastewater B	1	7.59 ± 0.02	118±16	855.0 ± 1.4	140.42 ± 0.4	168 ± 14	42.8 ± 0.6	38 000 000 ± 6 200 000
Well water	1	6.93 ± 0.01	122±4	631.5 ± 2.1	121.86 ± 0.77	24 ± 2	22.6 ± 0.5	5 500 000 ± 410 000
E. coli	29	7.4*	n.d.	n.d.	n.d.	n.d.	n.d.	1 200 000 000*

n.d. = not determined, *see the preparation method.

2.2. Contamination experiments

In the eight contamination experiments, each with a single contaminant and varying concentrations, five different types of contaminants including non-artificial contaminants (stormwater, treated wastewater, wastewater and well water) and a reference microbial contaminant (*E. coli*), were injected into the drinking water (Table 1). The non-artificial contaminants were filtered prior to injections through 100 μm nylon filters to homogenize them and avoid clogging the flow-imaging and light-scattering particle counter. The stormwater was sampled from a stormwater pipe, at the edge of a suburban area (Hervanta, Tampere, Finland), after rain in June. The incoming wastewater and effluent were 24-hour composite samples collected from a municipal wastewater treatment plant (Viinikanlahti, Tampere). The well water, meant for watering plants, was sampled in the proximity of an allotment garden in Tampere, Vuores. *E. coli* (strain MG1655) was prepared by cultivating cells overnight in Lysogeny broth medium supplemented with 0.4% glucose. The cells were collected by centrifugation and thereafter washed and resuspended in PBS buffer (pH 7.4). The solution of approximately $1.2 * 10^9$ cells/mL (optical density at 600 nm = 4) was vortexed gently before use. All of the contaminant samples were stored in the dark at 4 °C. The contamination experiments with each contaminant consisted of a set of 3–6 target concentrations, which included a range of supposedly undetectable concentrations in the low end and concentrations causing particle counter saturation in the high end (for details see **Table S1**). The target concentrations varied from the 0.0000083% v/v (100 cells/ml) of *E. coli* to the 3% v/v of treated wastewater B. Excluding the well water experiment, the experiments were performed stepwise: after a 29–35 min of injection, the injection pump was turned off for a period of 12–85 min. The well water experiment consisted of a single injection in which the well water concentration was increased after a period of time in the test environment by gradually increasing the well water concentration in the feeding container. All of the experiments were performed between 8 and 16 o'clock on working days to ensure the presence of water quality fluctuations.

On the day of the experiments, the filtered contaminants were diluted with the drinking water sampled from the same laboratory on the previous day and transferred to the feed containers no more than 60 min before the corresponding injection. This drinking water used for the dilution of the contaminants and as the reference feed was stored in tightly closed plastic containers at room temperature. Storing drinking water overnight reduced the free chlorine concentration by as much as by half, but its use in contaminant dilution did not impact the free chlorine concentration of the reference line during the experiments (approximately 5% of the water in both lines was feed). In addition, diluting the contaminant with the sampled drinking water decreased the chlorine concentration of the contaminant feed since chlorine oxidized the natural organic matter and microbes of the contaminant before the diluted contaminant was injected. These issues were considered unavoidable for two reasons. First, sampling dilution water during the experiments would have forced the use of dilution water with a possible high particle concentration due to water quality fluctuations. Second, the removal of chlorine from the sampled drinking water by volatilization into the air was considered too time-consuming. The chlorine was deliberately removed from the test environment in the *E. coli* experiment by dissolving approximately 0.3 g/L of sodium thiosulfate pentahydrate into the dilution water.

2.3. Online instrumentation

The online instrumentation of the study consisted of two types of particle counters and four conventional online water quality sensors as described in Table 2. The studied particle counters included a flow-imaging particle counter (A development version of Qumo water quality monitoring station, Uponor Corporation, Finland) and a light-scattering particle counter (OLS50P water with scattered light sensor SLS-25/25, PAMAS Partikelmess- und Analysesysteme GmbH, Germany), which worked as a reference particle counter to gain knowledge of particle concentrations and size distributions during the experiments. The conventional water quality sensors, later referred to as the sensors, included turbidity (Turbimax CUS51D), free chlorine (Memosens CCS51D), conductivity (Memosens CLS82D), and pH/ORP (Memosens CPS16D) sensors, all from Endress+Hauser, Switzerland. The placement of sensors and particle counters in the test environment is shown in Fig. 1.

During the study period, the maintenance of sensors and particle counters was instrument-specific. The flow cells of the flow-imaging particle counters were periodically flushed, except on the experiment days, and their windows were cleaned when deemed necessary by the inspection of the image quality. The light-scattering particle counter typically encountered clogging after running for 5–7 days, which resulted in zero responses in all channels. This was overcome by feeding 1 M of hydrochloric acid into the particle counter until the responses were stabilized. Before connecting the online particle counter back to the test environment, milli-Q water was fed into the particle counter for

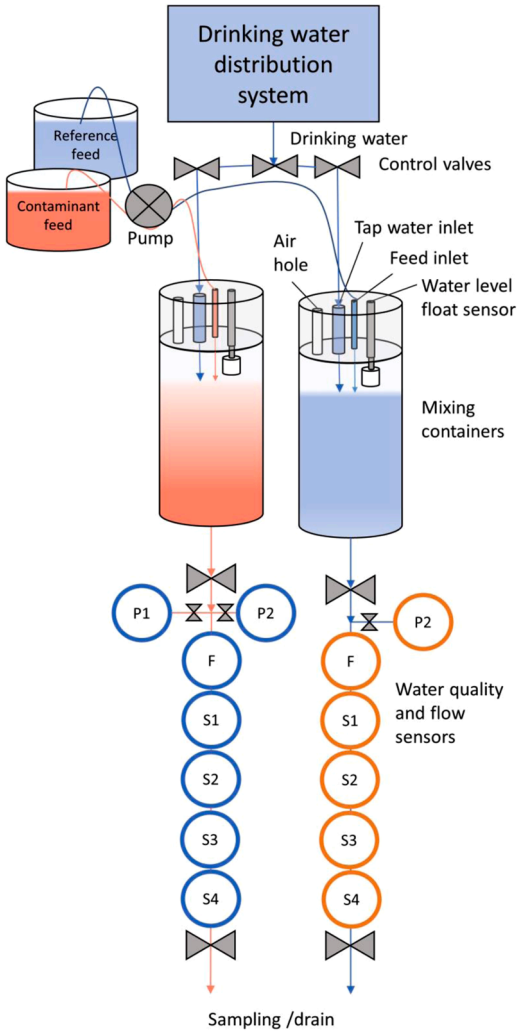

Fig. 1. Schematic representation of the test environment. The mixing container lid was a 3D-printed piece containing four holes for the air, drinking water, feed water and water level float sensor. The light-scattering particle counter (P1) and flow-imaging particle counter (P2) were installed after individual valves. The flowmeter (F) was installed prior to the sensor rack which included the turbidity (S1), free chlorine concentration (S2), conductivity (S3), and pH/ORP (S4) sensors.

at least 10 min. The conventional sensors were mechanically cleaned at the same time when the test environment was maintained. All of the sensors used factory calibration during the measurement periods. Turbidity results were later calibrated based on the turbidity of grab samples prior to the data analysis due to wall scattering issues observed in the 50 mm sensor rack. The sensor measurements were manually processed, and the observed measurement artifacts due to faulty sensors or test environment maintenance were removed from the figures. When the measurement artifacts were present during an experiment, a corresponding sensor was completely left out from figures and further analysis.

The operating principle of the flow-imaging particle counter is shown in Fig. 2. The water flows through a transparent flow channel. Directly on one of the windows of the flow channel is an image sensor, which is illuminated from the other side by a diverging beam from a pulsed diode laser (wavelength 405 nm). The particles suspended in the water scatter the light forward in an expanding cone. The scattered light interferes with the unscattered light and forms holograms on the image sensor. The images are captured continuously, and the particle holograms are detected, counted, and analyzed to classify the particles by the software embedded in the particle counter.

The software used internally literally thousands of measurement channels, but for simplicity, we reported the particle data collected into six measurement channels: N, B, C, F, Small, and Large, expressed as particles/mL Fig. 2. N-particles represent the total concentration of particles. Small (approx. < 1 μm) and Large (approx. > 2 μm) particle classifications resulted from estimating the particle size by the amplitude of the hologram and by comparison with the light-scattering particle counter. The B, C, and F classifications resulted from a hybrid machine-learning model combining several deep neural networks trained on data obtained prior to the contamination experiments with stormwater (Uponor R&D, unpublished).

Since the B, C and F classifications stem from neural networks, their properties cannot easily be described in terms of usual morphological parameters. However, sample images of the particles are shown in **S2 Figure S8** and some practical descriptions are given below. B-particles are larger than a few micrometers and tend to be irregularly shaped. They are often found in pipe sediment set loose by, for example, sudden flow changes in DS (Uponor R&D, unpublished). F-particles are fiber-like, i.e., they are much longer than they are wide. C-particles do not appear in normal pipe sediment and are more indicative of particles in stormwater or wastewater (Uponor R&D, unpublished). Due to properties of the classification algorithm used at the time of the experiments, a given particle can in principle belong simultaneously to C and either B or F classes, since the C classification results from a different algorithm than the B and F classifications. In addition, a particle in the Large class can simultaneously belong to any of B, C or F classes.

2.4. Analyses

To determine the water quality similarity in the contamination and reference lines on the days of the experiments, drinking water grab

Table 2
Online instrumentation and their characteristics in the study. The measuring interval was 3 min for the flow-imaging particle counter, 1 min for the light-scattering particle counter and 10 s for the conventional sensors. The inflow to the flow-imaging particle counter was 50–100 mL/min (measured volume > 2 mL, typically ~15 mL in 3 min) while that to the light-scattering particle counter was 10 mL/min (measured volume 10 mL).

Instrument	Measuring principle	Measuring range	Maximum measured error/accuracy
Flow-imaging particle counter	Digital holographic microscopy	0.7–100 μm, 6 measurement channels	n.a.
Light-scattering particle counter	Light-scattering	0.5–20 μm, 8 size channels; 0–13 000 particles/ml	7.8% (coincidence rate in max particle concentration)
Conductivity	Potentiometric	1 μS/cm – 500 mS/cm	<= 4%
Free chlorine concentration	Amperometric	0–20 mg/L	+- 2%
Oxidation reduction potential	Potentiometric, Ag/AgCl reference electrode	−1500–1500 mV	+- 5 mV
Turbidity	Nephelometric	0.000–4000 NTU	< 2% or 0.1 FNU
pH	Potentiometric, Ag/AgCl reference electrode	1–12	+- 0.028 pH
Temperature	Platinum resistance	−5–120 °C	n.a.

n.a. = not available.

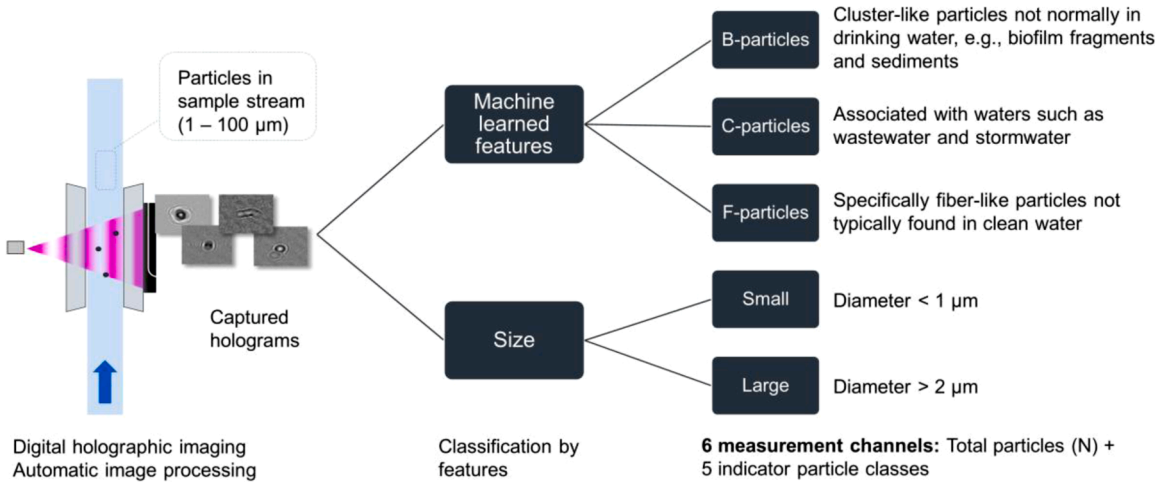

Fig. 2. The measurement and data processing principle of the flow-imaging particle counter.

samples were characterized for pH, oxidation–reduction potential (ORP), turbidity, conductivity, free chlorine concentration, and dissolved organic carbon (DOC). The grab samples of drinking water were taken in 500–1000 mL Pyrex bottles from the effluent tube in the test environment simultaneously from both lines no more than two hours prior to the first contaminant injection. These were stored in the dark at 4 °C and analyzed in two steps. First, pH and free chlorine were analyzed immediately after sampling. Second, ORP, conductivity, turbidity and DOC were analyzed within six hours of sampling.

ORP and pH were analyzed with a WTW pH 315i using WTW Sentix 41 and SI Analytics Blueline 31 RX electrodes, respectively. Conductivity measurements were performed with a WTW inoLab Cond Level 1 with a WTW TetraCon 325 electrode and turbidity measurements were performed with a WTW Turb 555. For free chlorine, a DPD reagent (Hach DPD Free Chlorine Reagent for 10 mL samples) was mixed with a 10 mL drinking water sample and measured by a Hach DR1900 portable spectrophotometer. DOC was measured according to EN 1484 1997 with a Shimadzu TOC-V_{CPH} instrument.

The characterization of filtered contaminants included the same aforementioned analyses as those for drinking water and, in addition, the filtered contaminants including stormwater, treated wastewater, wastewater and well water were analyzed for total suspended solids (TSS) according to standard procedure EN 872 2005 (filters, Whatman GF/C 1.2 µm) within 24 h from the first injection.

2.5. Signal-to-noise ratio of online measurements

The water quality signals of all of the sensors and particle counters were analyzed to assess sensor/class responses (later referred to as sensor responses) caused by the contaminant injections and to determine a limit of detection (LOD) for each sensor. The analysis consisted of calculating a mean difference of sensor response between a period of contaminant injection (a period in which the feed pump was on) and a period of a selected baseline. The mean difference was used in two methods. In the first method, a relative difference was calculated by dividing the difference by the mean of a selected baseline response to make it comparable between sensors/classes. The linearity of the relative difference in comparison to contaminant concentration was evaluated by calculating the linear regression coefficients of determination (R^2) using Python (v. 3.8.3) library Scikit-learn (v. 0.23.1) and its LinearRegression class. In the second method, the mean difference was extended to a signal-to-noise ratio (SNR) by dividing the resulting difference by the standard deviation of the selected baseline response (Szabo et al., 2008). Unlike Szabo et al. (2008), the baseline sensor response was selected via two approaches: (1) a corresponding reference line sensor response during each injection was used for the flow-imaging particle counter and conventional water quality sensors; (2) a contamination line sensor response after each experiment, namely 18–21 o'clock, was used to evaluate the first approach and to compare the responses of the flow-imaging and light-scattering particle counters. An SNR depicts a standardized and unitless difference of a sensor response. A positive SNR indicates that sensor response increases due to contaminant injection, whereas a negative SNR indicates that sensor response decreases due to contaminant injection. The following representation was used in this study:

$$SNR = \frac{\mu_{cont} - \mu_{ref}}{\sigma_{ref}} \quad (1)$$

where μ_{cont} is the mean of the sensor response caused by contaminant injection in the contamination line, μ_{ref} is the mean of the selected baseline sensor response and σ_{ref} is the standard deviation of the selected baseline sensor response. For example, Eq. (1) results in an SNR of 3 if the difference, $\mu_{cont} - \mu_{ref}$, is $3^*\sigma_{ref}$.

Even though the same water was fed into the contamination line and the reference line, the sensor responses were occasionally different due to apparent differences in sensor quality (for example ORP in Fig. 3), which are related to sensor accuracy (Table 2). This led to occasionally absolute SNR values of 3 in the control periods (no contaminant, 18–21 o'clock) (for details, see **Table S4**), which was overcome by selecting a conservative LOD value $|SNR| = 10$. To assume the identical baseline fluctuations for both lines, the sensor and flow-imaging particle counter responses of both lines were subsequently adjusted to the same initial level based on the sensor responses 20 min prior to the first injection of an experiment.

2.6. The relative proportions of particle classes and sizes

The relative proportions of different particle classes of the flow-imaging particle counter and size classes of the light-scattering particle counter for the different contaminants were determined as follows. First, the absolute concentration differences between the contamination and reference line (or the reference period for the light-scattering instrument) were determined at one of the higher concentrations of the experiment, but not always the highest concentration to avoid artefacts due to saturation of the instruments. Then, the baseline-subtracted concentrations were divided by that of the summary class of the instrument, namely, N or Total, to obtain the relative proportions of the particle classes.

For drinking water, the relative proportions of particle classes and

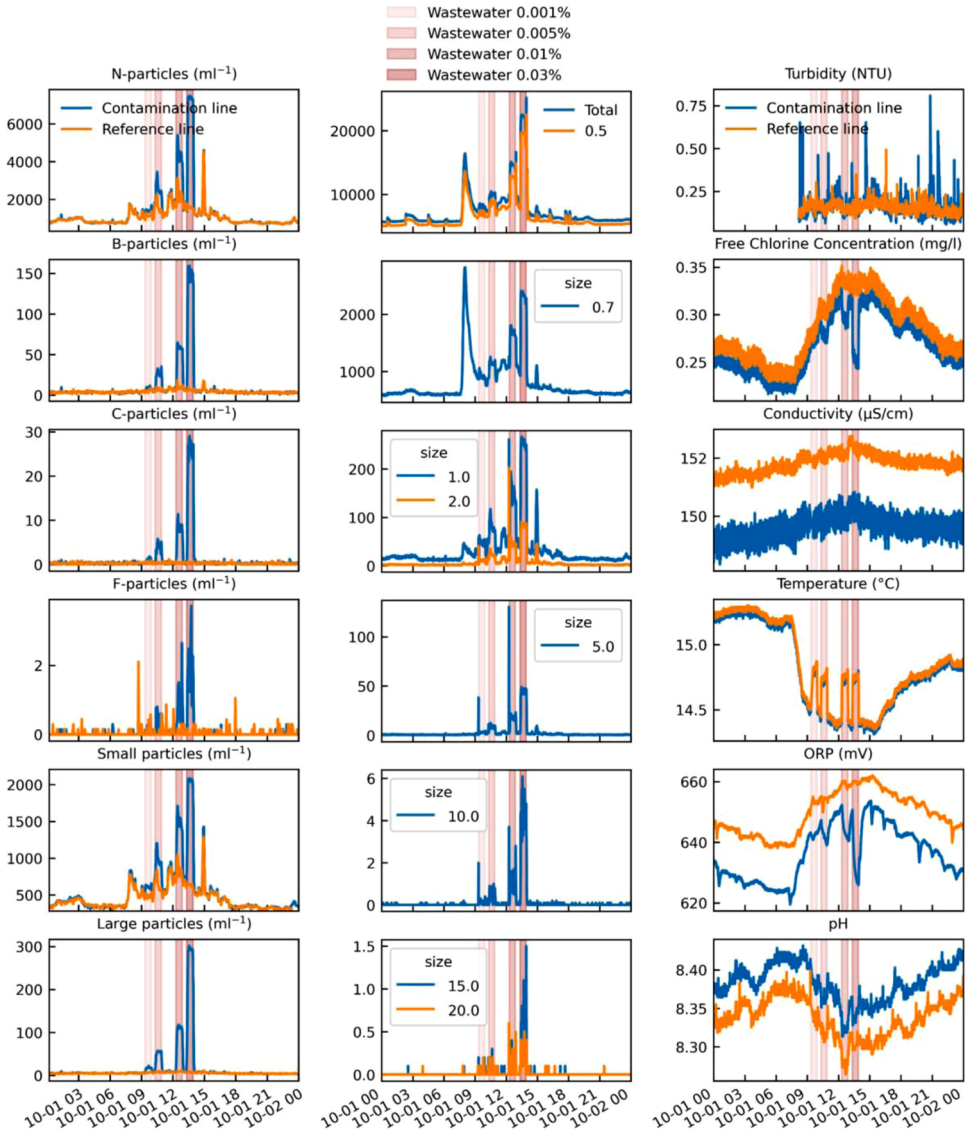

Fig. 3. The measurement data for the wastewater B experiment. The flow-imaging particle counter (left column) and conventional sensors (right column) measured both lines simultaneously whereas the light-scattering particle counter (middle column) measured only the contamination line. The horizontal axes depict the time in the format 'month-day hour'.

sizes were calculated from data collected at the experiment site during the first experiment period (Jun 2nd – Jul 16th, 2020). For the flow-imaging particle counter, the reference line instrument was used, while the only light-scattering particle counter available to us was installed in the contamination line. For every time point of this six-week data, the particle (size) class concentrations were divided by the respective summary class (N or total) to obtain the relative particle proportions. From this proportion data, the 25th and 75th percentiles were calculated. Since the light-scattering instrument was in the contamination line, the raw data also included the contamination periods, washings of the systems etc. We estimated that these exceptional times represented much less than 25% of the total measurement time and chose a safe upper limit of 75th percentile in order to obtain normal limits of fluctuation not affected by the known contaminations.

3. Results and discussion

3.1. Normal water quality fluctuations

In the present study, normal water quality fluctuations were determined for the 24-hour periods on the experiment days in order to separate the response to contaminants from the response to normal water quality fluctuations. These fluctuations were assessed for the flow-imaging particle counter and conventional water quality sensors.

The concentration of particles was higher during working hours (7–18 o'clock), especially in the morning, than at other times of the day, which was assumed to be caused by the rapid increase in water demand in the DS and surrounding property. For example, in Fig. 3, the total number of particles (N-particles) and Small particles measured by the flow-imaging particle counter fluctuate strongly in both lines also when contaminants are not added, especially between 7 and 18 o'clock. The N-particles in the reference line between 7 and 18 o'clock had a mean of 1367 mL^{-1} (39% std, $n = 220$); whereas, outside of these hours, the mean was 822 mL^{-1} (11% std, $n = 254$). In contrast, B, C, F and Large particle concentrations fluctuated visibly considerably less than N-particle concentrations(Fig. 3). Similarly, the light-scattering particle counter in the contamination line outside the contaminant additions recorded considerably larger concentration fluctuations for particles up to 1—2 µm than for the larger ones (Fig. 3, middle column).

The fluctuations in water quality measured by of the conventional

sensors, except for turbidity and conductivity, started around 7 o'clock and continued until midnight. Typically, free chlorine concentration and ORP fluctuations manifested a similar trend: They decreased from midnight to the morning hours and then increased until achieving a peak value between 9 and 18 o'clock. The pH was typically inversely proportional to the free chlorine concentration and ORP. Temperature fluctuations were occasionally very similar to free chlorine concentration, ORP, and pH (Fig. 3). Turbidity fluctuations were similar to the particle concentration fluctuations. Conductivity showed no daily fluctuations; typically, it showed an increasing/decreasing trend.

Daily fluctuations of water quality in a DS are known to be related to varying water demand since the alternating high flow during the day and low flow during the night may lead to the mobilization and accumulation of particulate material in pipes (Nescerecka et al., 2014; Prest et al., 2016; Sunny et al., 2020). In addition, the changes in the residence time in a DS may lead to varying temperatures, chlorine concentrations, pH, etc., in a DS, which likely explain the observed occasional similarity between temperature, free chlorine, ORP and pH fluctuations. Other explanations for the origins of water quality fluctuations include changes on water supply operation and maintenance and construction work in the water supply (Prest et al., 2016). The observed quality fluctuations in the present study were most likely related to the water demand of the property and the DS, indicating that the fluctuations were not caused by sensor artifacts or produced from the test environment in which the water flow was gravitational and constant.

3.2. *Sensor responses to wastewater and detection limits*

Contamination detection of the flow-imaging particle counter and conventional sensors was studied in the presence of normal water quality fluctuations by injecting different contaminants in various concentrations into one line of the continuously running test environment and analyzing simultaneously collected measurement data from both contamination and reference line. As discussed in Section 3.1, water quality fluctuations were present on all experiment days, as detected with all particle counters and sensors except for conductivity. The sensor responses to the contaminants were sudden positive (particle concentrations, turbidity) or negative (free chlorine concentration, ORP, pH) shifts to a new range, which lasted until the contaminant left the test environment (Fig. 3).

The magnitudes of the shifts caused by contaminant injections were determined as the relative differences between the contamination and reference lines, which were calculated by dividing the difference between contamination and reference line by the reference line value for all contaminants (**Table S3**). To evaluate how identical the two similar sensors/flow-particle counters performed in the two lines, the relative differences were calculated for the control period between 18 and 21 o'clock (marked as 0 mg/L concentration) in which no contaminant was injected. Wastewater experiment B was selected as an example to illustrate the differences in sensor responses due to the high particulate and dissolved content of the wastewater compared to the drinking water (Table 1). The high particulate content in the wastewater increased the

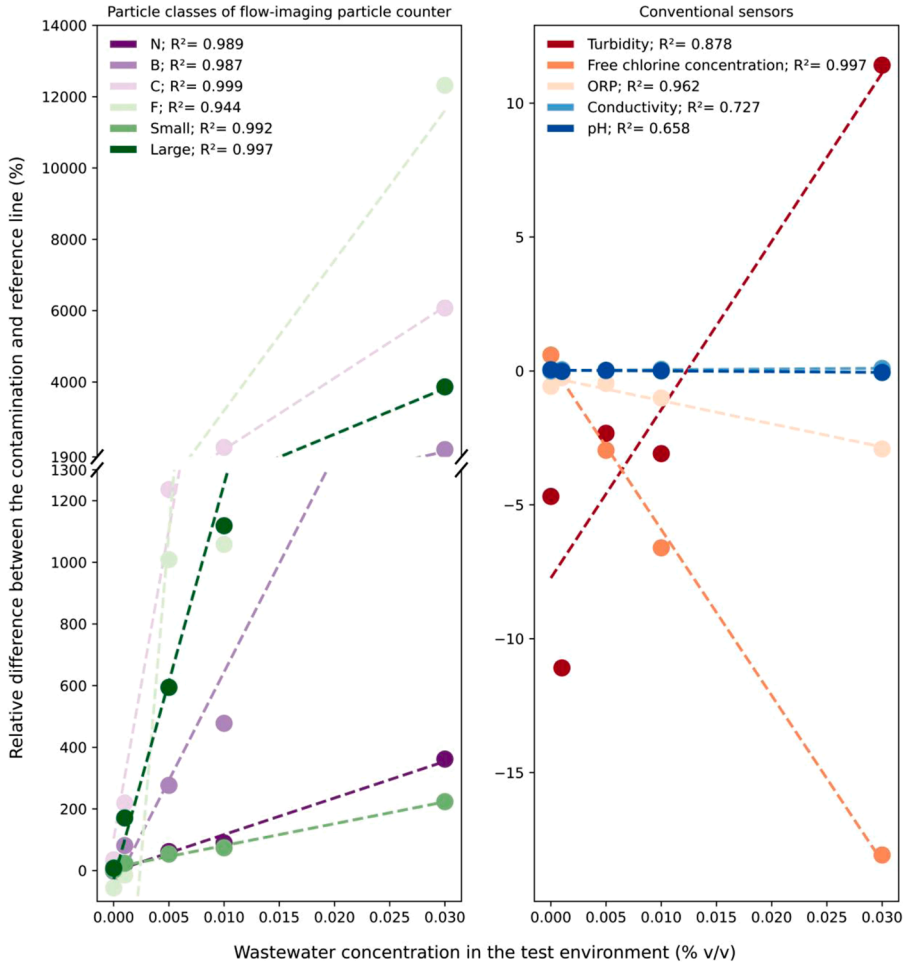

Fig. 4. Relative differences in the sensor responses of flow-imaging particle counter and conventional sensors to addition of wastewater concentrations in Wastewater B experiment. The relative difference was determined by dividing the difference of the contamination and reference line responses by the reference line response. The coefficient of determination (R^2) shows how well the observed values (o) are replicated by the linear model (–).

particle concentration and turbidity of the water in the contamination line. Thus, the relative differences were positive and increased linearly with wastewater concentration (R^2 = 0.878–0.999) (Fig. 4). By far, the steepest slope of the linear fit is observed for F- and C- particles, followed by Large and B- particles, while the relative responses of N (total) and Small particles and turbidity are substantially weaker. As seen in Fig. 3 and discussed in more detail in Section 3.4, very few F- and C- particles normally are present in drinking water, however, they do exist in wastewater, making the relative difference large. In contrast, due to a high number of small particles in drinking water, the relative increase in N, Small and turbidity caused by the contamination is considerably smaller.

Contrary to parameters measuring the particle content directly, free chlorine concentration and ORP decreased linearly with wastewater concentration (R^2 = 0.962–0.997). This is attributed to the particulate content of the wastewater consuming the free chlorine (ORP is a chlorine concentration surrogate) and the 5-fold lower ORP value of the wastewater compared to that of the drinking water (Table 1). The sensors for temperature, pH, and conductivity did not respond to the wastewater injection at the studied concentrations.

The difference between the contamination and reference line responses were extended to take into account the magnitude of normal water quality fluctuations by determining a signal-to-noise ratio (SNR), which was calculated by dividing the mean difference between the contamination line and reference line by the standard deviation of the reference line. SNR was used to determine the limit of detection value

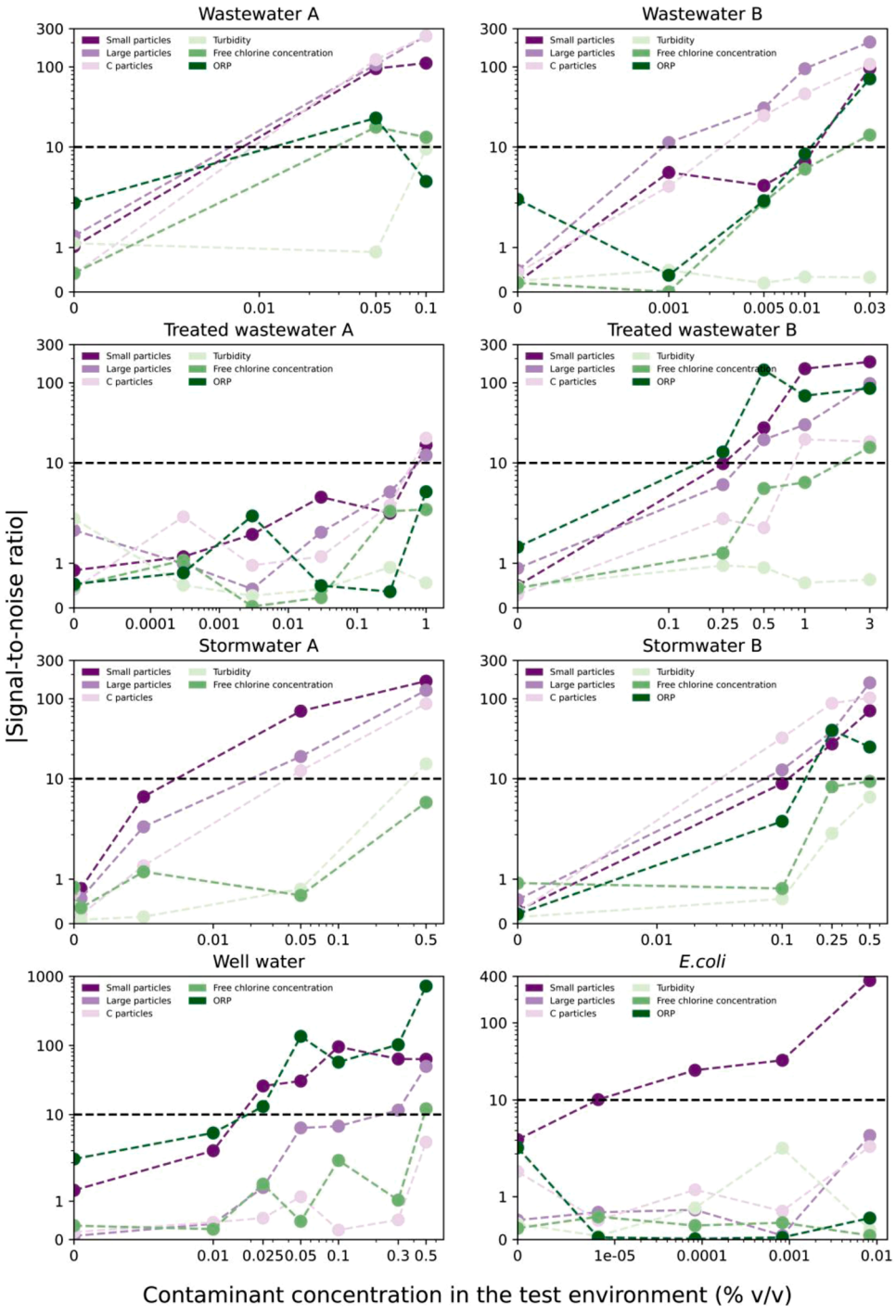

Fig. 5. Selected flow-imaging particle counter class (purple) and conventional sensor (green) responses in relation to the contaminant concentrations in all of the contamination experiments. The responses were determined as signal-to-noise ratios (SNRs), which describes the number of times the response exceeded the standard deviation of the reference line. The limit of detection value was set to |SNR| = 10 (black). Note that the vertical and horizontal axes start with a linear range which changes to a logarithmic range. (For interpretation of the references to color in this figure legend, the reader is referred to the web version of this article.)

(LOD) of the classes/sensors for a contaminant concentration by setting the LOD to $|SNR| = 10$, which indicates the response of ten times the standard deviation of the reference line. Even though the relative responses were typically linear (Fig. 4) after the LOD had been exceeded (Fig. 5, wastewater B), the SNR responses varied due to normal water quality fluctuations. To demonstrate the importance of taking normal water quality fluctuations into account in order to avoid overestimating the detection performance of difference classes/sensors, SNRs were determined by using the reference line as a baseline and using a period of 18–21 o'clock of the contamination line when no contaminants were injected as a baseline. The utilization of the reference line showed, for example, that the 0.01% wastewater B injection increased the mean N-particles by 2173 particles/mL (90%) (Fig. 4) in the flow-imaging particle counter in contamination line compared to that of the reference line. However, the corresponding standard deviation of the reference line (440 particles/mL) varied due to water quality fluctuations. Thus, the SNR was 5, remaining below the LOD (for all contaminants and injections, see **Table S2–S4**). In contrast, using only the contamination line data and thus the baseline period outside the working hours (a mean of 18–21 o'clock in the contamination line), can result in too optimistic LOD, shown as an increase in the mean N-particles in the contamination line by 3813 particles/mL (486%), with an SNR of 94 (for all contaminants and injections, see **Table S5–S7**). Due to the high standard deviation of the N-particles in the reference line during the injections, the SNR surpassed the LOD only for the highest concentration (0.03%) (**Table S4**), while the baseline period using only contamination line data indicated that even the 0.001% wastewater B injection was detectable (**Table S7**).

The use of the reference line in the test environment allowed for the analysis of sensor performance, mimicking realistic conditions such as those in DS. In comparison, previous pilot-scale drinking water contamination detection studies have concentrated on eliminating normal water quality fluctuations by recirculating drinking water (Besmer et al., 2017; Hall et al., 2007; Helbling and VanBriesen, 2008; Szabo et al., 2008) in the test environment rather than determining sensor performance in the presence of fluctuations. In an actual EWS, a reference line is not available and a baseline period must be estimated based on the already measured data; however, the present study highlighted that normal water quality fluctuations should be considered in improving contamination detection.

3.3. Impact of contaminants and their characteristics to sensor responses and detection limits

To investigate the flow-imaging particle counter and conventional sensor responses to different contaminants in the presence of normal water quality fluctuations, a total of 33 injections with eight contaminants were analyzed for the absolute values of SNRs. The classes of flow-imaging particle counter and turbidity were selected to analyze the responses to the particle content of contaminants. As a simplified illustration, Fig. 5 shows only the classes of Small, Large and C-particles (for all particle classes, see **Table S4**). The Small particles (< 1 μm) of the flow-imaging particle counter detected all of the studied contaminants by the criterion that SNR exceeded 10 (Fig. 5), similarly than the N-particles (total). In turn, the Large particles (> 2 μm) detected all of the studied contaminants except for the reference microbial contaminant (*E. coli)* by the criterion that SNR exceeded 10 (Fig. 5). The C-particles showed similar response to Large particles, however, the number of C-particles in the studied contaminants were considerably smaller than that of Large particles (see for example, Fig. 3). In addition, LOD was not exceeded for well water and *E.coli* contaminants. The particle classes are discussed in more detail in Section 3.4. The turbidity sensor could detect contamination for one of the highest suspended solid (TSS) concentrations of all of the injections based on the contaminant concentration (0.5% stormwater A). In this case TSS of stormwater was 29 mg/L on average (Table 1), resulting in a 0.15 mg/L TSS concentration in the water flowing through the contamination line. Moreover, the LOD almost (9.4) exceeded the 0.1% wastewater B injection, which lead to 0.16 mg TSS/L. For these two injections, the Small and Large particles exceeded the LOD in a 2–10-fold lower contaminant concentration with up to a 11-fold higher SNR in comparison to those of turbidity. Turbidity was not measured for the other high TSS concentration injections, namely, 3% treated wastewater B and 0.5% well water (**Table S1**).

The sensors responding to the consumption of chlorine, i.e., free chlorine concentration and ORP, can be considered as measuring both dissolved content as well as particulate content indirectly when the particulate content is assumed to consist of microorganisms or particulate organic matter, both of which are oxidized by chlorine. The free chlorine sensor could detect the highest concentrations of the filtered contaminant types (stormwater, treated wastewater, wastewater and well water) as indicated by exceeding the LOD for all of them except for the stormwater (0.5% stormwater B; SNR: 9.2) (Fig. 5). The LOD of the ORP sensor was up to 4 times lower than those of the free chlorine sensor.

In addition to ORP and free chlorine, the dissolved content in the contaminants was measured by conductivity and pH sensors. The conductivity responded to one of the highest dissolved solid concentrations (measured as conductivity) in drinking water of all of the injections, based on the contaminant concentration (0.3% treated wastewater A) and the contaminant conductivity (971 μS/cm). The response of pH sensor to contaminants did not exceed the LOD in these experiments.

The Small particle class was able to detect *E. coli* (Fig. 5), which was not possible for the conventional sensors tested. Previous studies (Hall et al., 2007; Ikonen et al., 2017) have suggested that turbidity responds to *E.coli* concentrations 1.6–10-fold higher than those in the present study, indicating that the sensitivity of the turbidity and other conventional sensors for detecting individual microorganisms from drinking water is one-thousandth of the sensitivity of the flow-imaging particle counter. The concentrations of *E. coli* in the present study are very high in comparison to typical drinking water quality guideline of 1 cells/100 mL and the studied particle counters cannot separate bacteria from other particles. In this respect flow cytometry outperforms particle counters.

The conventional sensors typically exceeded the LOD only at the highest studied contaminant concentrations or not at all, which indicates that higher contaminant concentrations would have been needed to determine LOD for conventional sensors. In the literature, for example, Szabo et al. (2008) injected 0.8% (v/v) unchlorinated secondary effluent from the wastewater treatment plant, with characteristics likely similar to treated wastewater A and B in the present study, into the pilot-scale test environment running chloraminated drinking water (2 mg/L), which resulted in the following relative responses and SNRs: conductivity 3.7% (SNR: 28.4), ORP 4.8% (SNR: 6.2), pH 0.5% (SNR: 7.2), and turbidity 116% (SNR: 23.1). The conductivity response was in line with that in the present study (treated wastewater A), while the turbidity response was considerably higher, which might be related to the selection of the baseline period or to the performance of the individual sensors. The low response of the ORP compared to the responses of the present study might have resulted from the chloraminated drinking water, in which the free chlorine is not present. Even though ORP has been considered to be a surrogate for the free/total chlorine concentration (Hall et al., 2007), the high SNR values of the ORP in the present study compared to those of the free chlorine suggest that the other dissolved constituents also play a role. The ORP had a relatively slow response to the contaminants compared to other sensors. For example, **S2 Figure S5** shows that the reference line had not returned to the normal level after injecting 0.1% wastewater $A + 0.3$ g/L thiosulfate, thus leading to an ORP value below the LOD.

The responses of different sensors and particle counters to contaminants in drinking water are heavily dependent on the characteristics of the drinking water (chlorination, water source, treatment process) and contaminants as well as fluctuations in the quality of drinking water. In general, the particle content of the drinking water is strictly regulated.

For instance, the Drinking Water Directive (European Union, 2020) regulates the effluent water of drinking water plants. Thus, the reference value of the treatment plants producing over 10000 m^3/day is set to 0.3 NTU in 95% of the samples, and none to exceed 1 NTU. On the other hand, the dissolved content of the drinking water is not considered a threat to public health similar to that of pathogens, and it varies more except in terms of chlorine concentration and pH, which are used to maximize the effectiveness of disinfection and reduce the pipe corrosion. Even though the ORP and conductivity sensors seem to respond considerably to contaminants in drinking water, they might not be suitable sensors for all kinds of DS. To illustrate, drinking water deriving from several water sources results in a high ORP and conductivity fluctuations depending on in what ratios water is fed to DS. However, in the studied DS, the conductivity did not fluctuate, while other sensors and the most classes of particle counters did, thus making conductivity suitable option for an EWS. The sensor selection for an EWS should be conducted based on the comparison of existing water quality data as well as preliminary online measurements in which the sensor responses to normal fluctuations are determined for different sensors. The present study showed that the use of conventional sensors for detecting contaminants from drinking water might still be convenient in applications in which sensitivity is not the highest priority.

3.4. The different particle classes as indicators for contamination

Since the flow-imaging particle counter classifies the particles in drinking water into six classes, namely, N, B, C, F, Small, and Large (Fig. 2), based on particle characteristics such as size and shape, the effect of particle class onto detection performance was further studied.

It was illustrated in Fig. 4 and discussed in Section 3.2 that in wastewater B experiment, the relative responses of the flow-imaging particle counter classes (C, F, B, Large) were considerably larger than those of the N- or Small particles. The light-scattering particle counter results corroborated this observation by recording substantially greater relative increases in the concentrations of larger particles (>1600% for particles > 1 μm) than those of small particles (<270% for particles < 1 μm), using the 0.03% (v/v) injection as an example (**Table S6**). This result was quite general: during injections with stormwater, treated wastewater and wastewater, the relative increases of the particles larger than 1 μm, as measured with the light-scattering particle counter, and the B-, C-, F-, and Large particles of the flow-imaging particle counter (**Table S3**), were manifold compared to the relative increases of particles smaller than 1 μm and the N-, Small particles. At most concentrations with stormwater and treated or untreated wastewater, the C-particles showed the greatest relative concentration changes of all flow-imaging particle classes. With well water and *E. coli*, however, the largest relative changes were observed for the Small particles at most concentrations.

To understand why the relative concentrations of certain particle classes increase more rapidly than others when a contaminant is added, it is useful to compare the relative compositions of the contaminant and drinking water. In Fig. 6, the relative abundances of particle classes, characterized by both the flow imaging and light-scattering particle counters, are shown for the studied contaminants. In essence, Fig. 6 shows the resulting relative particle class or size distribution if the contaminant were injected to ultrapure water with no particles at all. This facilitates comparison between the different contaminants. Moreover, Fig. 6 shows the limits of normal fluctuation of drinking water shown as a shading between the 25th and 75th percentiles.

The key to understanding Fig. 6 is to look whether the relative proportion of a particle class in a contaminant is considerably above the normal range of pure drinking water. If so, that particle class may be a good indicator for that contaminant. The above condition was true for stormwater, treated wastewater and wastewater with particle classes B, C, F and Large and for particle sizes larger than 1 μm. Well water and *E. coli* particle class distributions were different by having substantially higher proportion of Small particles and lower proportion of B-, C-, F- and Large particles than the other contaminants. With the light-scattering particle counter, the distinction was less clear, but still apparent, well water and *E. coli* have a high proportion of the smallest particles and a very low proportion of particles larger than 5—10 μm.

The SNR did not generally follow the same trend as the relative increase. For the flow-imaging particle counter using the reference line as a baseline, only in the following cases was the SNR higher for a specific

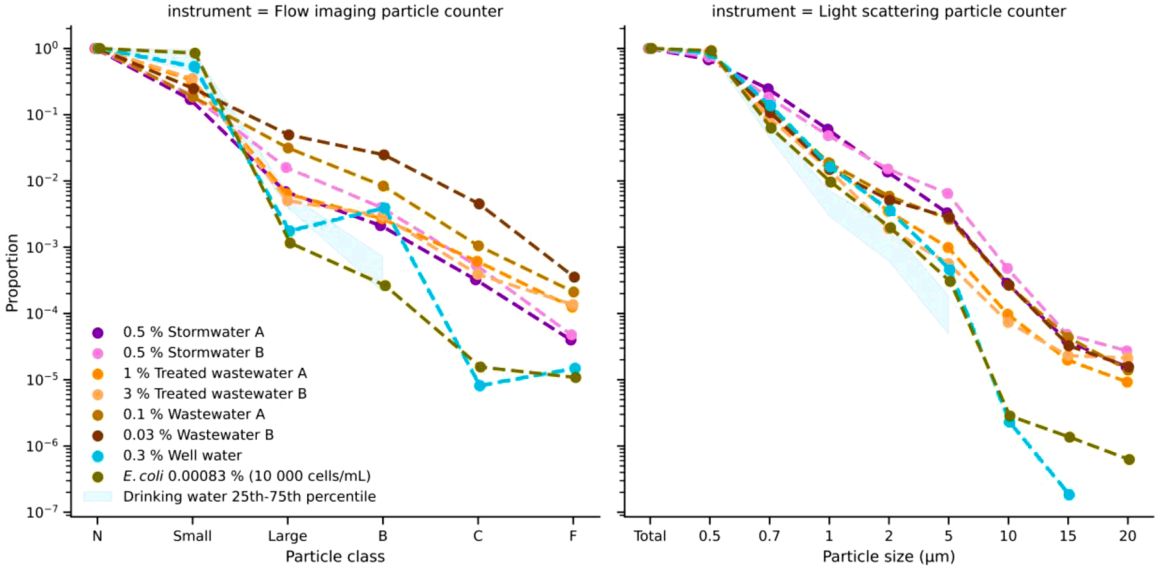

Fig. 6. The relative particle class/size distribution of the studied contaminants and drinking water determined by the flow-imaging particle counter (left) and the light-scattering particle counter (right). The drinking water particle size distribution was calculated from the period Jun 2nd – Jul 16th, 2020 and is shown as the blue shading spanning the 25th and 75th percentiles. Since even the 75th percentile was 0 for the C and F classes and for particle sizes larger than 10 μm, the shading cannot be shown on the logarithmic proportion scale. The particle sizes on the right indicate the lower bound of the size bin. For example, 0.5 means particles 0.5—0.7 μm, and 2 means particles 2—5 μm. (For interpretation of the references to color in this figure legend, the reader is referred to the web version of this article.)

particle class than for both the N and Small particles: Stormwater B (0.1%, 0.25%) (C-particles), wastewaters A and B (C, Large and B particles) (**Table S4**). For the light-scattering particle counter, the SNR for particles larger than 1 μm was higher than that for particles smaller than 1 μm in the following cases: stormwater A and B, wastewater A (>5 μm) and wastewater B. (**Table S7**). The reason for the apparent discrepancy between the relative concentration increase and the SNR may lie in the statistics. Large particles were quite rare both in the reference line or during baseline measurement, and during the rather dilute contaminations. Therefore, the standard deviation in the denominator of the SNR equation (Eq. (1)) is relatively large compared with the absolute concentration difference, making the SNR smaller. The SNRs at all contaminant concentrations are listed in **Table S4** for the flow-imaging particle counter and conventional sensors, and in **Table S7** for the light-scattering particle counter, and are shown graphically for selected parameters in Fig. 5. From that data it can be gleaned, for example, that in most cases for stormwaters, treated wastewaters and wastewaters, whenever the SNR for N- or Small particles exceeded 10, so did also the SNR for B-, C- or Large particles.

To illustrate the feasibility of machine-learned particle classes, namely, B, C, and F, their contamination detection performance was further analyzed. Although the relative proportion of B-particles was considerably higher than that of C-particles for all the studied contaminants (Fig. 6), the C-particles may be a better contamination indicator, since also pure drinking water contains B-particles. The B-particles might represent sediment particles that occasionally detach and are transported in a DS. Curiously, the well water was visually rusty and contained a considerable number of B particles (Fig. 6). The high content of iron and manganese was confirmed by laboratory analyses (results not shown). The fiber-like F-particles were still substantially rarer than C-particles in the studied stormwater, wastewater and treated wastewater contaminants (Fig. 6), which limited their usefulness as generic contamination indicator. However, the distinct shape of F-particles may help to identify certain types of contaminants.

Recent research on drinking water contamination monitoring has mainly focused on online microbial monitoring (Besmer et al., 2017; Favere et al., 2021); however, a particle size range of 1–8 μm has been proposed for detecting contaminants in general in DS (Ikonen et al., 2017). Microbial content tends to fluctuate due to varying hydraulic conditions, water temperature, water source, and treatment (Prest et al., 2016), which was shown in the present study to be true also for particle sizes smaller than 10 μm. The present study suggests that the relative proportion of larger particles in pure drinking water is low based on the particle concentration observation of six weeks (Fig. 6), where 75% of the time less than 0.7% of particles were in size range 1—2 μm, less than 0.2% 2—5 μm, and less than 0.02% larger than 5 μm. On the smaller end of the size spectrum, 75% of the time more than 90% of particles were in size range 0.5—0.7 μm and more than 4.4% between 0.7 and 1 μm. Comparing relative particle size distributions obtained using different instruments may not be straightforward, if the LOD (smallest detectable particle size) or the size bins differ. With this in mind, the above finding generally agrees with observations from various Danish drinking water DSs, in which less than 0.1% of particles were larger than 5 μm (Højris et al., 2016), probably due to downstream water treatment processes such as sand filtration and activated carbon filtration as mentioned in Section 3.3. However, the larger particles in DSs have been observed in more downstream locations (Prest et al., 2021; Verberk et al., 2006) and they have been associated with discoloration events (Vreeburg et al., 2008). Since the test environment of the present study was located only two kilometers away from the treatment plant, the observed fluctuations of larger particles may be less than those of further down the DS. For future studies, it might be useful to determine if the particle classes of the flow-imaging particle counter could also detect discoloration events.

To distinguish real contamination events from normal water quality fluctuations, in general, one should select parameters that have a high relative response to contaminants and a low response to normal water quality fluctuations. An ideal parameter candidate has a response proportional to the contaminant concentration (for the sensor in the contamination line) and a flat profile otherwise (Fig. 3 and **Table S2–S7**). The C- and F-particle classes of the flow-imaging particle counter, and classes for particles larger than 10 μm (light-scattering particle counter) seem to be most specific to contamination by stormwater and wastewater. The Small and N-particle classes and those pertaining to particles smaller than 2 μm are catch-all parameters that responded to the studied contaminants in addition to normal fluctuations. The B-particle class was hypothesized to be associated with sediment particles, that may be regarded as an indicator for non-harmful discoloration events and not actual contamination. Of the conventional water quality sensors, only conductivity was relatively immune to normal quality fluctuations, but it only responded strongly to treated wastewater. For parameters that respond to both contaminants and normal fluctuations, one needs to utilize detection algorithms that are able to eliminate the effect of normal water quality fluctuations; however, normal water quality fluctuations can be somewhat irregular due to their nature, which can in turn lead to false alarms in an EWS.

4. Conclusions

- The simultaneous and continuous baseline measurements during contaminant injections made it possible to separate sensor responses caused by contaminants from those caused by normal water quality fluctuations present in a DS. Not taking into account normal quality fluctuations may lead to overestimating a sensor's capability to detect contaminants.
- Normal water quality fluctuations impacted the responses of the particle classes N, Small, Large, B of the flow-imaging particle counter, particle size classes less than 10 μm of the light-scattering particle counter as well as the conventional sensors except conductivity.
- Particle classes C and F of the flow-imaging particle counter and particle sizes >10 μm of the light-scattering particle counter were relatively immune to normal water quality fluctuations, in addition to that they had a high relative response to contaminations with stormwater and wastewater.
- Small particle class of the flow-imaging particle counter and the < 1 μm classes of the light-scattering particle counter detected all the studied contaminants, including those with an especially high content of small particles (well water and *E. coli*), however, they were susceptible to normal water quality fluctuations.
- ORP, which responded both to dissolved and particulate contaminants, detected the presence of all of the studied contaminants, except *E. coli*.

Declaration of Competing Interest

The authors declare that they have no known competing financial interests or personal relationships that could have appeared to influence the work reported in this paper.

Acknowledgements

This work was supported by the Kaute Foundation - The Finnish Science Foundation for Economics and Technology and Uponor Corporation. We thank Esa Hämäläinen for help in the experiment planning stage as well as Mika Karttunen and Antti Nuottajärvi for their practical contribution to the test environment. Uponor Corporation acknowledges collaboration with Emblica Oy on developing the machine learning models. In addition, we would like to thank Zeinab Ahmed and Kati Rintala for their help in the laboratory as well as Suvi Santala for her contribution to the preparation of the *E.coli* solution.

Supplementary materials

Supplementary material associated with this article can be found, in the online version, at doi:10.1016/j.watres.2022.118149.

References

Besmer, M.D., Sigrist, J.A., Props, R., Buysschaert, B., Mao, G., Boon, N., Hammes, F., 2017. Laboratory-scale simulation and real-time tracking of a microbial contamination event and subsequent shock-chlorination in drinking water. Front. Microbiol. 8, 1900. https://doi.org/10.3389/fmicb.2017.01900.

Besner, M.C., Prévost, M., Regli, S., 2011. Assessing the public health risk of microbial intrusion events in distribution systems: conceptual model, available data, and challenges. Water Res. 45, 961–979. https://doi.org/10.1016/j.watres.2010.10.035.

Dejus, S., Nescerecka, A., Kurcalts, G., Juhna, T., 2018. Detection of drinking water contamination event with Mahalanobis distance method, using on-line monitoring sensors and manual measurement data. Water Sci. Technol. Water Supply 18, 2133–2141. https://doi.org/10.2166/ws.2018.039.

EN 1484, 1997. Water analysis. Guidelines for the determination of total organic carbon (TOC) and dissolved organic carbon (DOC). European committee for standardization.

EN 872, 2005. Water quality. Determination of suspended solids. Method by filtration through glass fibre filters. European committee for standardization.

European Union, 2020. Directive (EU) 2020/2184 of the European Parliament and of the Council of 16 December 2020 on the quality of water intended for human consumption (recast) (Text with EEA relevance).

Favere, J., Waegenaar, F., Boon, N., De Gusseme, B., 2021. Online microbial monitoring of drinking water: how do different techniques respond to contaminations in practice? Water Res. 202, 117387 https://doi.org/10.1016/j.watres.2021.117387.

Hall, J., Zaffiro, A.D., Marx, R.B., Kefauver, P.C., Radha Krishnan, E., Haught, R.C., Herrmann, J.G., 2007. On-line water quality parameters as indicators of distribution system contamination. J. /Am. Water Work. Assoc. 99, 66–77. https://doi.org/10.1002/j.1551-8833.2007.tb07847.x.

Helbling, D.E., VanBriesen, J.M., 2008. Continuous monitoring of residual chlorine concentrations in response to controlled microbial intrusions in a laboratory-scale distribution system. Water Res. 42, 3162–3172. https://doi.org/10.1016/j.watres.2008.03.009.

Højris, B., Christensen, S.C.B., Albrechtsen, H.-J., Smith, C., Dahlqvist, M., 2016. A novel, optical, on-line bacteria sensor for monitoring drinking water quality. Sci. Rep. 6, 23935. https://doi.org/10.1038/srep23935.

Højris, B., Kornholt, S.N., Christensen, S.C.B., Albrechtsen, H.-J., Olesen, L.S., 2018. Detection of drinking water contamination by an optical real-time bacteria sensor. H2Open J. 1, 160–168. https://doi.org/10.2166/h2oj.2018.014.

Ikonen, J., Pitkänen, T., Kosse, P., Ciszek, R., Kolehmainen, M., Miettinen, I.T., 2017. On-line detection of Escherichia coli intrusion in a pilot-scale drinking water distribution system. J. Environ. Manage. 198, 384–392. https://doi.org/10.1016/j.jenvman.2017.04.090.

Laine, J., Huovinen, E., Virtanen, M.J., Snellman, M., Lumio, J., Ruutu, P., Kujansuu, E., Vuento, R., Pitkänen, T., Miettinen, I., Herrala, J., Lepistö, O., Antonen, J., Helenius, J., Hänninen, M.L., Maunula, L., Mustonen, J., Kuusi, M., Collin, P., Korpela, M., Kuusela, A.L., Mustajoki, S., Oksa, H., Räsänen, S., Uotila, T., Katto, T., 2011. An extensive gastroenteritis outbreak after drinking-water contamination by sewage effluent, Finland. Epidemiol. Infect. 139, 1105–1113. https://doi.org/10.1017/S0950268810002141.

Larsson, C., Andersson, Y., Allestam, G., Lindqvist, A., Nenonen, N., Bergstedt, O., Institute of Biomedicine, D. of I.M., Institutionen för biomedicin, avdelningen för infektionssjukdomar, 2014. Epidemiology and estimated costs of a large waterborne outbreak of norovirus infection in Sweden. Epidemiol. Infect. 142, 592–600. https://doi.org/10.1017/S0950268813001209.

Liu, S., Che, H., Smith, K., Chang, T., 2015. A real time method of contaminant classification using conventional water quality sensors. J. Environ. Manage. 154, 13–21. https://doi.org/10.1016/j.jenvman.2015.02.023.

Liu, S., Che, H., Smith, K., Chen, L., 2014. Contamination event detection using multiple types of conventional water quality sensors in source water. Environ. Sci. Process. Impacts 16, 2028–2038. https://doi.org/10.1039/c4em00188e.

Liu, S., Li, R., Smith, K., Che, H., 2016. Why conventional detection methods fail in identifying the existence of contamination events. Water Res. 93, 222–229. https://doi.org/10.1016/j.watres.2016.02.027.

McKenna, S.A., Wilson, M., Klise, K.A., 2008. Detecting changes in water quality data. J. /Am. Water Work. Assoc. 100, 74–85. https://doi.org/10.1002/j.1551-8833.2008.tb08131.x.

Mellou, K., Katsioulis, A., Potamiti-Komi, M., Pournaras, S., Kyritsi, M., Katsiaflaka, A., Kallimani, A., Kokkinos, P., Petinaki, E., Sideroglou, T., Georgakopoulou, T., Vantarakis, A., Hadjichristodoulou, C., 2014. A large waterborne gastroenteritis outbreak in central Greece, March 2012: challenges for the investigation and management. Epidemiol. Infect. 142, 40–50. https://doi.org/10.1017/S0950268813000939.

Nescerecka, A., Rubulis, J., Vital, M., Juhna, T., Hammes, F., 2014. Biological instability in a chlorinated drinking water distribution network. PLoS One 9, e96354. https://doi.org/10.1371/journal.pone.0096354.

Ozcan, A., McLeod, E., 2016. Lensless imaging and sensing. Annu. Rev. Biomed. Eng. 18, 77–102. https://doi.org/10.1146/annurev-bioeng-092515-010849.

Prest, E.I., Hammes, F., van Loosdrecht, M.C.M., Vrouwenvelder, J.S., 2016. Biological stability of drinking water: controlling factors, methods, and challenges. Front. Microbiol. 7 https://doi.org/10.3389/fmicb.2016.00045.

Prest, E.I., Schaap, P.G., Besmer, M.D., Hammes, F., 2021. Dynamic hydraulics in a drinking water distribution system influence suspended particles and turbidity, but not microbiology. Water (Switzerland) 13. https://doi.org/10.3390/w13010109.

Pronk, M., Goldscheider, N., Zopfi, J., 2007. Particle-size distribution as indicator for fecal bacteria contamination of drinking water from karst springs. Environ. Sci. Technol. 41, 8400–8405. https://doi.org/10.1021/es071976f.

Rhoads, W.J., Garner, E., Ji, P., Zhu, N., Parks, J., Schwake, D.O., Pruden, A., Edwards, M.A., 2017. Distribution system operational deficiencies coincide with reported Legionnaires' Disease clusters in Flint, Michigan. Environ. Sci. Technol. 51, 11986–11995. https://doi.org/10.1021/acs.est.7b01589.

Ripple, D.C., DeRose, P.C., 2018. Primary determination of particle number concentration with light obscuration and dynamic imaging particle counters. J. Res. Natl. Inst. Stand. Technol. 123 https://doi.org/10.6028/jres.123.002.

Safford, H.R., Bischel, H.N., 2019. Flow cytometry applications in water treatment, distribution, and reuse: a review. Water Res. 151, 110–133. https://doi.org/10.1016/j.watres.2018.12.016.

Sunny, I., Husband, P.S., Boxall, J.B., 2020. Impact of hydraulic interventions on chronic and acute material loading and discolouration risk in drinking water distribution systems. Water Res. 169, 115224 https://doi.org/10.1016/j.watres.2019.115224.

Szabo, J., Hall, J., Meiners, G., 2008. Sensor response to contamination in choloraminated drinking water. J. /Am. Water Work. Assoc. 100, 33–40. https://doi.org/10.1002/j.1551-8833.2008.tb09606.x.

Verberk, J.Q.J.C., Hamilton, L.A., O'Halloran, K.J., Van Der Horst, W., Vreeburg, J., 2006. Analysis of particle numbers, size and composition in drinking water transportation pipelines: results of online measurements. Water Sci. Technol. https://doi.org/10.2166/ws.2006.902.

Vreeburg, J.H.G., Schippers, D., Verberk, J.Q.J.C., van Dijk, J.C., 2008. Impact of particles on sediment accumulation in a drinking water distribution system. Water Res. 42, 4233–4242. https://doi.org/10.1016/j.watres.2008.05.024.

Whelton, A.J., McMillan, L.K., Connell, M., Kelley, K.M., Gill, J.P., White, K.D., Gupta, R., Dey, R., Novy, C., 2015. Residential tap water contamination following the freedom industries chemical spill: perceptions, water quality, and health impacts. Environ. Sci. Technol. 49, 813–823. https://doi.org/10.1021/es5040969.

Xu, W., Jericho, M.H., Meinertzhagen, I.A., Kreuzer, H.J., 2001. Digital in-line holography for biological applications. Proc. Natl. Acad. Sci. U. S. A. 98, 11301–11305. https://doi.org/10.1073/pnas.191361398.